An easy-to-fabricate low-temperature TiO2 electron collection layer for high efficiency planar heterojunction perovskite solar cells

B. Conings, L. Baeten, T. Jacobs, R. Dera, J. D'Haen, J. Manca, and H.-G. Boyen

Citation: APL Materials **2**, 081505 (2014); doi: 10.1063/1.4890245
View online: http://dx.doi.org/10.1063/1.4890245
View Table of Contents: http://scitation.aip.org/content/aip/journal/aplmater/2/8?ver=pdfcov
Published by the AIP Publishing

Articles you may be interested in

Influence of crystalline titanium oxide layer smoothness on the performance of inverted organic bilayer solar cells
Appl. Phys. Lett. **102**, 183903 (2013); 10.1063/1.4804599

The role of Ag nanoparticles in inverted polymer solar cells: Surface plasmon resonance and backscattering centers
Appl. Phys. Lett. **102**, 123301 (2013); 10.1063/1.4798553

Control of an interfacial MoSe2 layer in Cu2ZnSnSe4 thin film solar cells: 8.9% power conversion efficiency with a TiN diffusion barrier
Appl. Phys. Lett. **101**, 053903 (2012); 10.1063/1.4740276

Electronic structure of indium tin oxide/nanocrystalline TiO2 interfaces as used in dye-sensitized solar cell devices
J. Appl. Phys. **109**, 113719 (2011); 10.1063/1.3596544

Use of fluorine-doped tin oxide instead of indium tin oxide in highly efficient air-fabricated inverted polymer solar cells
Appl. Phys. Lett. **96**, 133506 (2010); 10.1063/1.3374406

AIP Journal of Applied Physics

Journal of Applied Physics is pleased to announce André Anders as its new Editor-in-Chief

This article is copyrighted as indicated in the article. Reuse of AIP content is subject to the terms at: http://aplmaterials.aip.org/about/rights_and_permissions Downloaded to IP: 37.201.224.142 On: Thu, 17 Jul 2014 17:27:10

APL MATERIALS **2**, 081505 (2014)

An easy-to-fabricate low-temperature TiO_2 electron collection layer for high efficiency planar heterojunction perovskite solar cells

B. Conings, L. Baeten, T. Jacobs, R. Dera, J. D'Haen, J. Manca, and H.-G. Boyen
Instituut voor Materiaalonderzoek, Universiteit Hasselt, Wetenschapspark 1, 3590 Diepenbeek, Belgium

(Received 30 April 2014; accepted 3 July 2014; published online 16 July 2014)

Organometal trihalide perovskite solar cells arguably represent the most auspicious new photovoltaic technology so far, as they possess an astonishing combination of properties. The impressive and brisk advances achieved so far bring forth highly efficient and solution processable solar cells, holding great promise to grow into a mature technology that is ready to be embedded on a large scale. However, the vast majority of state-of-the-art perovskite solar cells contains a dense TiO_2 electron collection layer that requires a high temperature treatment (>450 °C), which obstructs the road towards roll-to-roll processing on flexible foils that can withstand no more than ~150 °C. Furthermore, this high temperature treatment leads to an overall increased energy payback time and cumulative energy demand for this emerging photovoltaic technology. Here we present the implementation of an alternative TiO_2 layer formed from an easily prepared nanoparticle dispersion, with annealing needs well within reach of roll-to-roll processing, making this technology also appealing from the energy payback aspect. Chemical and morphological analysis allows to understand and optimize the processing conditions of the TiO_2 layer, finally resulting in a maximum obtained efficiency of 13.6% for a planar heterojunction solar cell within an ITO/TiO_2/$CH_3NH_3PbI_{3-x}Cl_x$/poly(3-hexylthiophene)/Ag architecture. © *2014 Author(s). All article content, except where otherwise noted, is licensed under a Creative Commons Attribution 3.0 Unported License.* [http://dx.doi.org/10.1063/1.4890245]

Since the first reports on hybrid solar cells based on organolead trihalide perovskites, these materials have thoroughly engrossed the photovoltaic community.[1,2] Already from the birth of this new class of solar cells, high photon-to-electron conversion efficiencies have been reported for cells containing either $CH_3NH_3PbI_3$ or $CH_3NH_3PbI_{3-x}Cl_x$, thereby almost immediately overtaking the record efficiencies of organic solar cells and dye-sensitized solar cells, and leading up to a current world-record of 17.9% in a matter of only a few years.[3] This fast-paced progress to such high efficiencies announces this new technology as a true potential rival for Si-based photovoltaics. In first instance, the perovskite was regarded as a new kind of dye that could boost the efficiency of dye-sensitized solar cells.[4,5] The dye is grafted onto a porous metal-oxide structure to optimize light absorption and simultaneously guarantee favorable charge transport. Therefore (and in unawareness of its true capabilities), the perovskite solar cell concept initially often inherited the porous metal-oxide structure, which at the same time would be ostensibly required to guarantee sufficiently large area for exciton dissociation.[6] However, not much later it was discovered that the typical three-dimensional organolead trihalide perovskites exhibit very high charge carrier diffusion lengths (especially for the mixed halide with Cl, up to >1 μm) and low exciton binding energy (<50 meV), while having a very high absorption coefficient and charge carrier mobility.[7–10] Moreover, it has been shown that the perovskite actually functions as the ambipolar layer in a p-i-n junction.[11] The combination of these observations raises serious doubts regarding the necessity of the well-established porous metal-oxide

 © Author(s) 2014

This article is copyrighted as indicated in the article. Reuse of AIP content is subject to the terms at: http://aplmaterials.aip.org/about/rights_and_permissions Downloaded to IP: 37.201.224.142 On: Thu, 17 Jul 2014 17:27:10

matrix in perovskite-based solar cells, even though there are many high efficiencies reported based on mesoporous TiO_2.[6,12–15] Indeed, several groups pointed out that a simpler device architecture, where a perovskite layer is sandwiched between selective contacts, is able to deliver comparable or even better performance than a mesoporous TiO_2/perovskite compound: Efficiencies of around 11% were obtained for solution-processed planar heterojunction $CH_3NH_3PbI_{3-x}Cl_x$-based solar cells, and even up to 15.4% by vapor deposition.[16–18] In the latter cases the compact TiO_2 layer was deposited by heating a precursor gel at high temperature (∼500 °C), lacking compatibility with flexible substrates and thus presenting a drawback in view of industrial scale roll-to-roll fabrication. This can in principle be remedied by using poly(3,4-ethylenedioxythiophene) polystyrene sulfonate (PEDOT:PSS) as bottom selective contact (thereby inverting the device structure),[19,20] though the hygroscopic nature of PEDOT:PSS would likely hamper the long-term stability of the moisture-sensitive perovskite.[21] It was then shown that the high temperature treatment for TiO_2 can be circumvented by using a layer consisting of TiO_2 nanoparticles, rather than one that is *in situ* formed by annealing a precursor gel. Two strategies have been demonstrated so far, either the deposition of a nanoparticle dispersion[22] or the direct precipitation of TiO_2 nanoparticles from solution onto the substrate.[23] Both methods use $TiCl_4$ as the titanium source, which produces HCl fumes when in contact with humidity and thus has to be handled with great care. Another method does use titanium isopropoxide (TIP) as titanium source, but requires the addition of graphene flakes to the resulting TiO_2 dispersion to obtain optimal performance.[24] Here we present the chemical and morphological characterization of a TIP-based sub-150 °C processed TiO_2 electron acceptor layer consisting of nanoparticles, and we investigate the influence of this layer on the morphology of the subsequently deposited perovskite layer. The nanoparticulate TiO_2 layer is deposited from an alcoholic dispersion that is very easy to synthesize and the resulting planar heterojunction solar cells outperform previously reported analogs containing high-temperature processed TiO_2 layers. The resulting maximum obtained conversion efficiency of 13.6% is to the authors' knowledge the highest reported value for a *solution processed* planar heterojunction solar cell based on mixed halide perovskite $CH_3NH_3PbI_{3-x}Cl_x$.

Our TiO_2 nanoparticle dispersion was prepared using a slight modification of a procedure reported by Katoch *et al.*[25] A 470 μl of TIP was added dropwise to a solution of 123 μl nitric acid in 2.5 ml ethanol under mild stirring. After stirring for 2 h, 114 μl of demineralized water was added for the hydrolysis to proceed and the solution was left stirring for another hour. The result was then diluted with 1-propanol. This transparent dispersion is ready for use, with no need for centrifugation, washing, and redispersing, and is stable for months (Figure 1(a): a 0.127 M dispersion). Fig. 1(b) shows a Dynamic Light Scattering (DLS) measurement of the dispersion, revealing a narrow size distribution with an average particle size of 6 nm. An X-ray diffraction (XRD) measurement of a dried powder sample is shown in Figure 1(c), confirming the anatase phase of the material, and confirming the crystal diameter measured with DLS (via Scherrer equation). Recently, it was shown by Wojciechowski *et al.* that the addition of a small amount of titanium diisopropoxide bis(acetylacetonate) (TiAcAc) to a TiO_2 dispersion can serve as "electronic glue" between the nanoparticles in the eventual nanoparticulate thin film, enhancing its conductivity and thus improving the resulting solar cell built on it.[22] In addition, the TiAcAc can also assist in the film formation itself. Figures 1(d)–1(f) show Atomic Force Microscopy (AFM) micrographs of 25–30 nm thin TiO_2 films spincoated on indium-tin-oxide (ITO) (3000 rpm; 1000 rpm/s; 30 s) from a 0.127 M dispersion with the addition of 8 mol.% of TiAcAc (0.08 mole of TiAcAc per mole of TiO_2), annealed for different times at 135 °C in air. Smooth films are obtained with a low root-mean-square roughness of 1 nm or less on ITO as base layer.

The thermally treated TiO_2-covered ITO substrates were then used to build planar heterojunction $CH_3NH_3PbI_{3-x}Cl_x$ perovskite solar cells according to a previously published procedure.[17] In short, a 3:1 methylammonium iodide:$PbCl_2$ solution in dimethylsulfoxide (DMSO) was spincoated (3000 rpm; 800 rpm/s; 540 s) on the TiO_2 in a nitrogen-filled glovebox, followed by a thermal treatment at 100 °C for 60 min. A layer of poly(3-hexylthiophene) (P3HT) (nominally 60 nm) was then spincoated on top, followed by the evaporation of 200 nm of silver at a pressure of 1×10^{-6} mbar to complete the devices. A key observation is the influence of the thermal treatment of the TiO_2 on the performance of otherwise identical solar cells. Devices made from unannealed TiO_2 exhibit a reasonable open-circuit voltage (V_{oc}) but a negligible short-circuit current (J_{sc}) and a very low fill

This article is copyrighted as indicated in the article. Reuse of AIP content is subject to the terms at: http://aplmaterials.aip.org/about/rights_and_permissions Downloaded to IP: 37.201.224.142 On: Thu, 17 Jul 2014 17:27:10

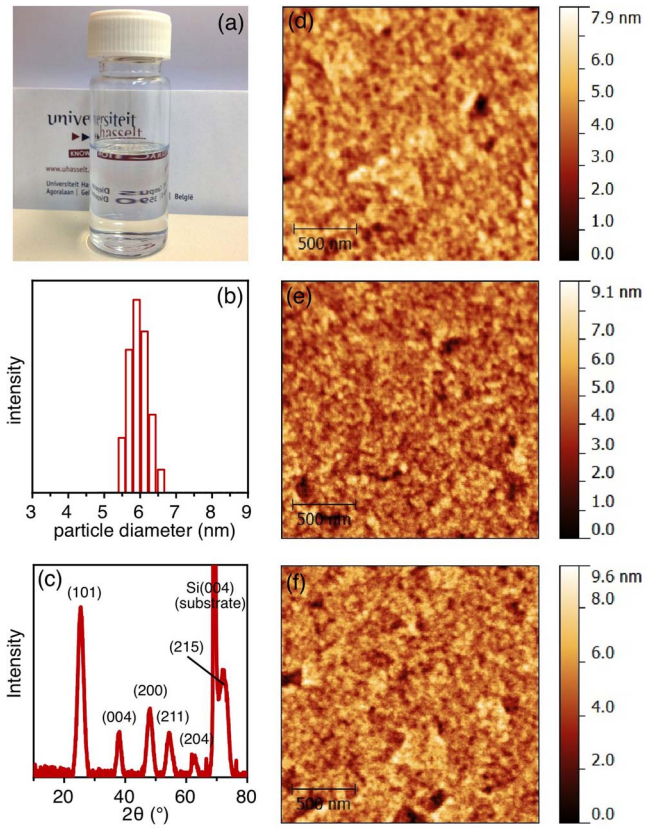

FIG. 1. (a) Photographic image of a bottle of TiO_2 dispersion with a concentration of 0.127 M. (b) DLS measurement of the TiO_2 dispersion. (c) XRD spectrum of a TiO_2 powder sample. (d)–(f) AFM images of a TiO_2 nanoparticulate layer on ITO with the addition of 8 mol.% TiAcAc prior to spincoating (2×2 μm), annealed in air at 135 °C for 10 min (d), 45 min (e), and 90 min (f).

factor (FF), resulting in close to zero photovoltaic output (Fig. 2(a)). The extremely low J_{sc} and FF indicate the presence of a very high series resistance, likely induced by the presence of precursor products. Indeed, when the TiO_2 is annealed at 135 °C for only 10 min, we already find a reasonable conversion efficiency of around 9%. J_{sc} keeps increasing with a longer TiO_2 thermal treatment, finding a maximum at 45 min, leading to an average efficiency of 12.6%. Efficiencies of even up to 13.6% (Fig. 2(b)) were obtained using an adapted annealing treatment as recently described by Saliba *et al.*, where the perovskite is slowly heated to 100 °C and then fast to 130 °C.[26] Longer TiO_2 treatments tend to have a vastly detrimental effect, initially resulting in highly fluctuating performance, and in the case of 90 min annealing even in a breakdown of all cells during the first measurement. It must not be overlooked that the best efficiencies obtained with our new low temperature processed TiO_2 layer are considerably higher than those obtained by using a sintered TiO_2 layer (500 °C) we reported before ($J_{sc} = 20.8 \pm 0.4$ mA/cm^2; $V_{oc} = 0.919 \pm 0.006$ V; FF = 0.54 ± 0.01; $\eta = 10.4 \pm 0.4$%).[17]

To find the origin of the performance dependence on the thermal history of the TiO_2 layer, chemical analysis of the layers was performed using X-ray photoelectron Spectroscopy (XPS). No other elements than the ones expected from the starting products (C, N, O, Ti) were found in the TiO_2 layers, confirming their chemical purity. To probe more into detail, high-resolution core level spectra were taken of relevant elements. Fig. 3(a) shows N1s spectra of TiO_2 layers that were annealed at 135 °C for times from 0 to 90 min. In the pristine case there are two clear components: a higher binding energy component that represents nitrates (407.5 eV) and a low binding energy component that corresponds with nitrogen in a carbonated environment (400.5 eV), resulting from nitric acid, and both TIP and TiAcAc, respectively.[27] As the TiO_2 layer is annealed, the nitrate component

This article is copyrighted as indicated in the article. Reuse of AIP content is subject to the terms at: http://aplmaterials.aip.org/about/rights_and_permissions Downloaded to IP: 37.201.224.142 On: Thu, 17 Jul 2014 17:27:10

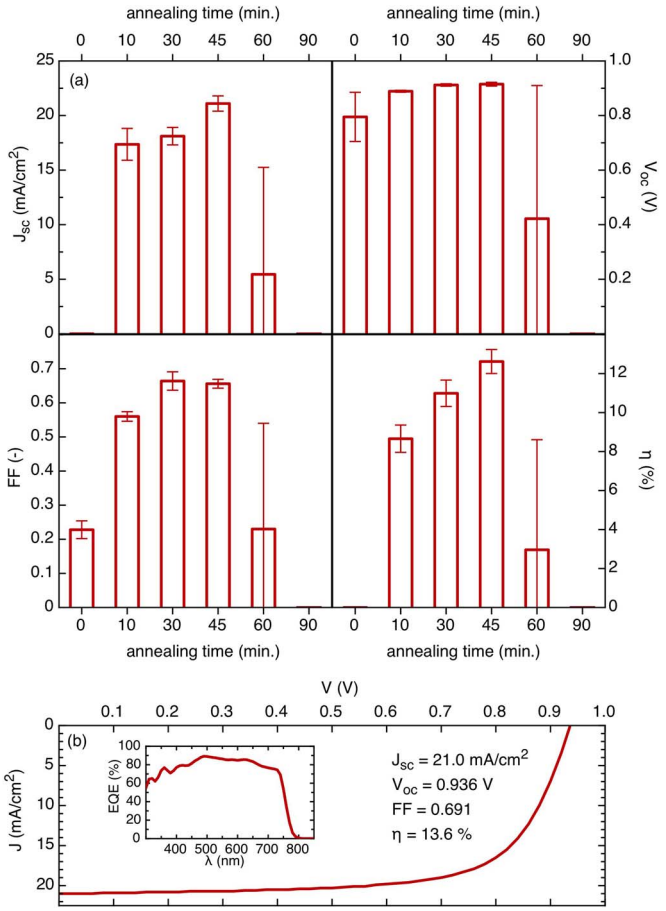

FIG. 2. (a) Photovoltaic parameters of a series of solar cells built on TiO_2 layers that were annealed for different times. Error bars represent the standard deviation of at least 4 cells. The large error bars for the case of 60 min of annealing reflect extreme fluctuations between individual cells, with occurrences of both shunting and decently performing cells. All cells were measured in the forward bias to J_{sc} direction after 10 min of AM1.5 illumination. (b) JV-characteristic of the best cell, using a 45 min annealed TiO_2 layer and a flash-anneal of the perovskite. Inset: External quantum efficiency spectrum.

shrinks, which is logical since the annealing temperature of 135 °C is well above the boiling point of nitric acid (83 °C). However, the nitrite component vanishes in favor of the component at lower binding energy, indicating that the nitric acid is disintegrated and its nitrogen being incorporated in the organic matrix of TiAcAc and TIP residue. This is seconded by the corresponding C1s core level spectra (Fig. 3(b)), as will be clarified in the following. The C1s comprises three components: one at 284.6 eV (C–C bonds), one at 286.8 eV (C–N and C–O bonds), and one at 289 eV (carboxyl).[27] We observe that the C–N/C–O component at 286.8 eV decreases upon annealing, while the carboxylic component at 289 eV increases; these are the organic moieties from the TIP and TiAcAc that oxidize due to the annealing being executed in air. The small remainder of the peak at 286.8 eV must therefore be a C–N contribution, corresponding with the nitrogen peak at 400.5 eV. Notice that the complete disappearance of nitric acid at 45 min of annealing coincides with the maximum obtained efficiency of the corresponding solar cells (Fig. 2(a)), indicating that the presence of residual nitric acid induces a parasitic series resistance in the device and could possibly cause interfacial recombination.

We turn our attention now to the Ti2p spectra in Fig. 3(c), comparing a pristine versus a 45 min annealed layer. It is immediately obvious that there is no elemental Ti present in either case (454 eV); all Ti is in the 4+ oxidation state (459 eV).[27] It has previously been speculated that TiAcAc might decompose upon heating, forming TiOx that acts as mortar between TiO_2 particles, thus increasing the resulting layer's conductivity.[22] While annealing does induce decomposition of the carbonated part of TiAcAc (as shown above), the presence of Ti in different oxidation states (e.g., 3+ or 2+)

This article is copyrighted as indicated in the article. Reuse of AIP content is subject to the terms at: http://aplmaterials.aip.org/about/rights_and_permissions Downloaded to IP: 37.201.224.142 On: Thu, 17 Jul 2014 17:27:10

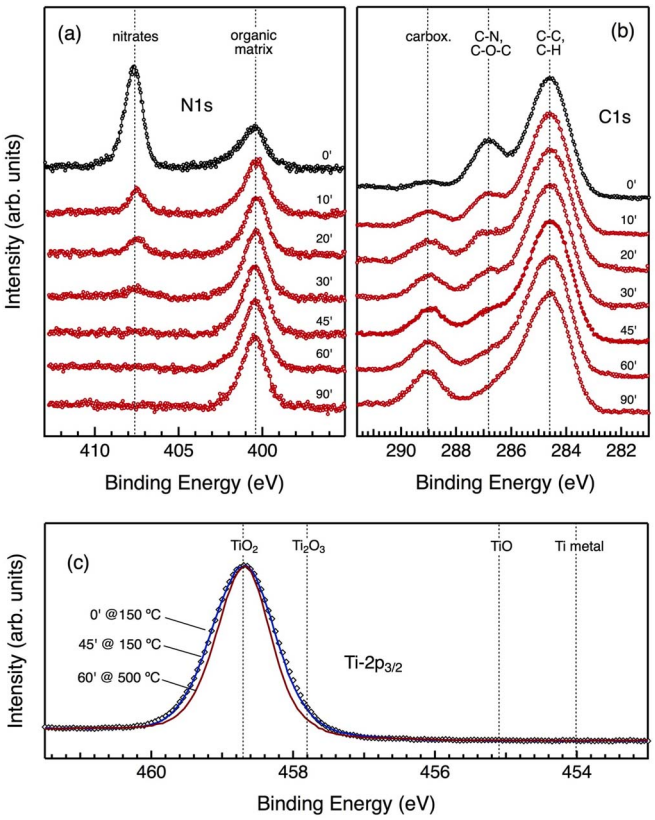

FIG. 3. (a) High-resolution N1s core level spectra of TiO_2 layers annealed for 0–90 min. (b) High-resolution C1s core level spectra of TiO_2 layers annealed for 0–90 min. (c) High resolution $Ti2p_{3/2}$ core level spectra of a TiO_2 layer before (diamonds) and after (blue line) annealing for 45 min at 135 °C together with a spectrum acquired on a TiO_2 layer sintered for 60 min at 500 °C (red line). For comparison, characteristic line positions of different oxidation states have been added.

should be corroborated by additional peaks appearing at the low binding energy side of the main line. In contrast, our measured $Ti2p_{3/2}$ signal comprising only a Ti^{4+} component that is unchanged upon annealing at 135 °C, reveals the absence of any Ti^{3+}[28] or Ti^{2+}[29] contributions to the spectrum. In fact, when analyzing the $Ti2p_{3/2}$ photoemission peak using a physically motivated line shape,[30] a single symmetric line turns out to be sufficient to describe the experimental data, thus ruling out the presence of any additional components with oxidation state other than 4+.

At this point one might speculate that a degraded form of TiAcAc with 4+ oxidation state for Ti is capable of bridging the voids between TiO_2 nanoparticles such that the resulting layer has a better conductivity. The source of an improved conductivity can indeed be traced back by comparing the $Ti2p_{3/2}$ core level region for a layer after annealing at 135 °C with that of a conventional TiO_2 sol-gel film sintered at 500 °C,[31] both measured under identical experimental conditions (Fig. 3(c)). Clearly, the low-temperature deposition induces a significant line broadening as compared to the sintered film. As the line shape of the latter represents the combined effects of (i) line broadening due to the finite life time of the photoionized states of the probed Ti ions and (ii) the broadening induced by the finite energy resolution of the spectrometer, the increased line width in case of the low-temperature sample clearly points to an additional broadening effect. This additional line broadening most likely arises from small fluctuations/deviations in stoichiometry around the probed Ti ions, which can best be expressed as $TiO_{2\pm\delta}$, reflecting a distribution of different ''chemically shifted'' components that superimpose to form the measured photoemission line. Consequently, a significant density of, e.g., defects acting as dopants must be present in the low-temperature deposited titania films, which can most probably be assigned to the "mortar" material, easily explaining their improved conductivity.

This article is copyrighted as indicated in the article. Reuse of AIP content is subject to the terms at: http://aplmaterials.aip.org/about/rights_and_permissions Downloaded to IP: 37.201.224.142 On: Thu, 17 Jul 2014 17:27:10

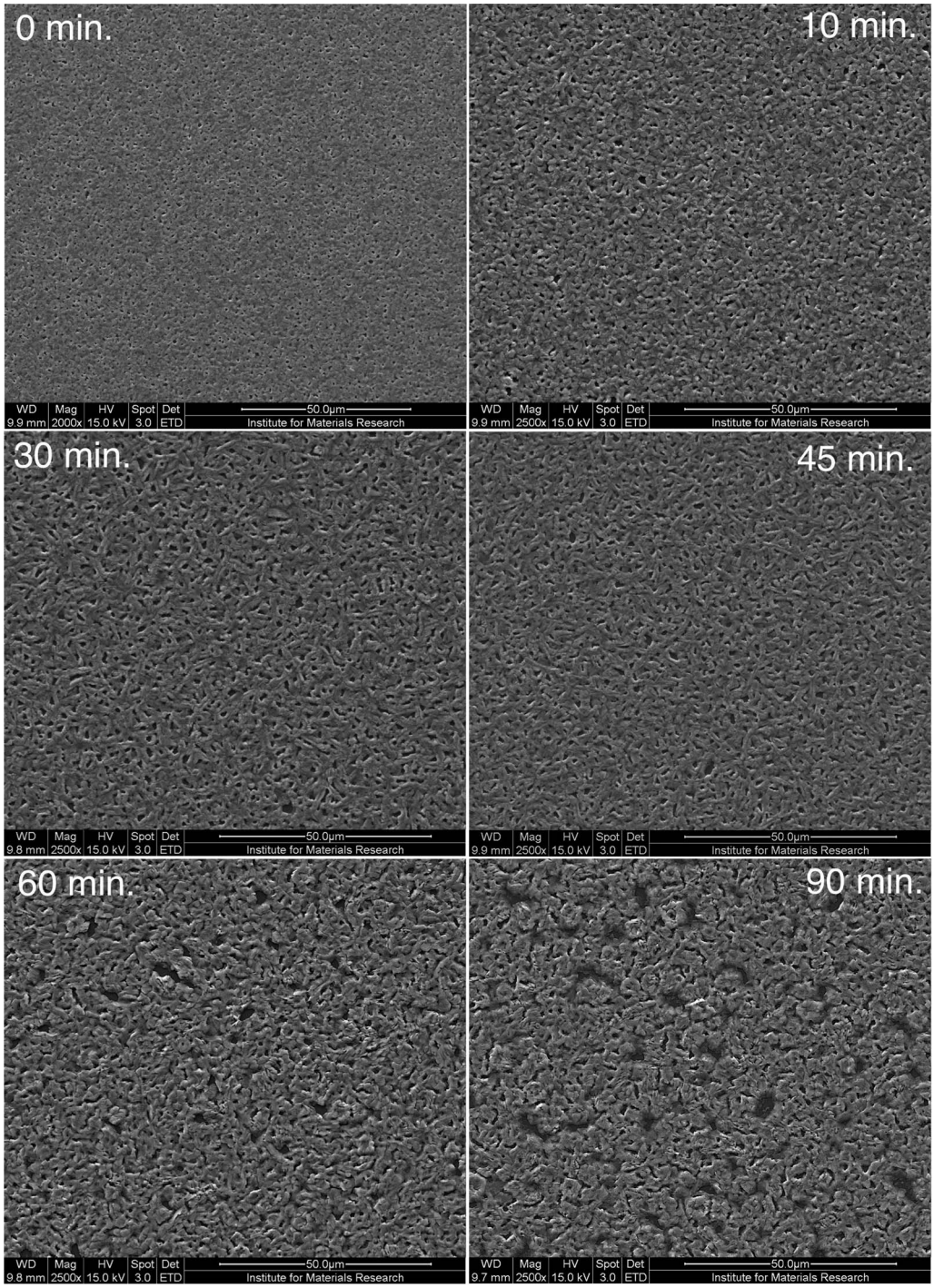

FIG. 4. SEM images of perovskite layers deposited on TiO_2 base layer that were annealed at 135 °C in air for different times from 0 to 90 min.

Based on the analysis of the N1s and C1s spectra it is clear why the TiO_2 layer needs a thermal treatment of 45 min to obtain optimally functioning solar cells (decomposition of NO_3), though it is still obscure why a longer annealing step results in much less performance and in worst-case even shunting cells. To shed more light onto the negative effect of prolonged annealing, we now examine the perovskite layer. Scanning Electron Microscopy (SEM) images were recorded to investigate

This article is copyrighted as indicated in the article. Reuse of AIP content is subject to the terms at: http://aplmaterials.aip.org/about/rights_and_permissions Downloaded to IP: 37.201.224.142 On: Thu, 17 Jul 2014 17:27:10

whether the annealing time could have an influence on the consecutively deposited perovskite. The series of images in Fig. 4 reveal that there is indeed a correlation between the thermal history of the TiO_2 and the morphology of the eventual perovskite layer. The smoothest layer is obtained for a pristine TiO_2 layer, however the photovoltaic properties are, as mentioned, overshadowed in this case by the detrimental presence of HNO_3. An intermediate annealing time of the TiO_2 (10–45 min) returns grainy to needle-like perovskite morphologies that closely resemble those we previously reported, accompanied by decent photovoltaic performance. Those films do show a number of pinholes but, contrary to foregoing hypotheses, this does not need to degrade the resulting performance significantly.[17] A treatment beyond 45 min appears to induce a considerably coarser perovskite morphology that shows much larger holes of several square micrometers. This is the likely cause why corresponding solar cells shunt easily; at such holes there is only a thin layer of P3HT (nominally 60 nm) that separates the TiO_2 from the top silver contact, so the occurrence of occasional short circuits is conceivable. It also deserves to be mentioned that the gradual change in morphology seen in the SEM results is paralleled by a decrease in peak height of the (hh0) peaks in XRD (not shown), indicating a reduced preferential orientation of the perovskite crystals. This might lead to inferior charge transport and could be an additional reason for the low performance of solar cells containing overly annealed TiO_2 layers.

The origin of the perovskite morphology dependence on the thermal history of the TiO_2 layer can be explained by the presented chemical analysis. The observed increased presence of carboxyl moieties on the TiO_2 surface as function of annealing time points to an enhanced wettability of the surface for the DMSO-based perovskite precursor, intuitively implying better film formation. In spite of that, the eventual perovskite layers show an opposite trend, becoming rougher when deposited on longer annealed TiO_2. This can be rationalized by considering that the actual perovskite is formed only when the precursor film is heated, i.e., the initial solvent wetting properties are subordinate to the subsequent crystallization mechanism of the dried film. As has been shown before, a high quality perovskite film is often more easily formed when a preformed matrix or a textured surface is available, functioning as a kind of seed layer.[11,32] Therefore, we propose that the organic residue from the starting products (at 286.8 eV in the C1s spectra in Fig. 3(b)) assists in the formation of smoother perovskite films. Upon the conversion into carboxylic compounds (at 289 eV), there are fewer seeding options for the perovskite crystals, causing them to form more rough and discrete structures, rather than an uninterrupted film.

Finally, it is interesting to remark that our extremely smooth anatase TiO_2 layers, having "minimal" contact area with the perovskite (i.e., a rather sharp bilayer interface), still allow for very high photocurrents. This is in contrast with a recent report from Yella *et al.*, who observe that rather rough rutile TiO_2 layers, having a more intimate contact with the perovskite, are more efficient at extracting electrons. An explanation for this apparent inconsistency might be offered by their use of the triiodide-based perovskite (that generally has lower charge carrier diffusion lengths) as opposed to the mixed halide variety in our case (typically with higher diffusion length).[7] In the former case a rougher TiO_2 film may assist in compensating for the slightly inferior charge carrier diffusion length of the triiode perovskite by creating an ersatz bulk heterojunction, whereas in the latter case any additional roughness would be redundant.

In conclusion, we introduced a low-temperature processable TiO_2 electron collection layer, customized for planar heterojunction perovskite solar cells. The layer is deposited from an easy one-pot synthesis nanoparticle dispersion and requires a thermal treatment at only 135 °C, in contrast with the typical 450 °C–500 °C baking steps for conventional TiO_2 base layers, making it compatible with roll-to-roll fabrication on plastic foils. Even slightly lower temperatures could deliver the same outcome, provided longer annealing times and/or lower pressure. In addition, the resulting planar heterojunction devices significantly outperform their otherwise identical counterparts containing a high temperature processed TiO_2 layer. From this initial set of experiments, an efficiency of 13.6% is achieved, which is at the time of writing the highest value for solution-processed planar heterojunction mixed halide perovskite solar cells so far, and the highest value for a perovskite solar cell using P3HT as hole transporting layer. The results also show that the chemical composition and thermal history of the nanoparticulate TiO_2 film have a consequential impact on the device

This article is copyrighted as indicated in the article. Reuse of AIP content is subject to the terms at: http://aplmaterials.aip.org/about/rights_and_permissions Downloaded to IP: 37.201.224.142 On: Thu, 17 Jul 2014 17:27:10

performance. Finally, it cannot go unnoticed that the observed high photocurrents and fill factors are obtained even with films exhibiting a significant amount of pinholes, illustrating that the interplay between the selective contact and the perovskite is probably an even more important consideration than the smoothness of the perovskite itself.

This work was financially supported by the Interreg project Organext and the Research Foundation Flanders (FWO) within the Odysseus program. B.C. is a postdoctoral fellow of FWO. The authors would like to acknowledge B. Ruttens for XRD measurement, T. Vandenreijt for technical assistance, and Aslihan Babayigit for extraordinary logistics.

[1] N.-G. Park, J. Phys. Chem. Lett. **4**, 2423–2429 (2013).
[2] H. J. Snaith, J. Phys. Chem. Lett. **4**(21), 3623–3630 (2013).
[3] NREL, see http://www.nrel.gov/ncpv/images/efficiency_chart.jpg, 2014.
[4] A. Kojima, K. Teshima, Y. Shirai, and T. Miyasaka, J. Am. Chem. Soc. **131**(17), 6050–6051 (2009).
[5] J.-H. Im, C.-R. Lee, J.-W. Lee, S.-W. Park, and N.-G. Park, Nanoscale **3**(10), 4088–4093 (2011).
[6] J. H. Heo, S. H. Im, J. H. Noh, T. N. Mandal, C.-S. Lim, J. A. Chang, Y. H. Lee, H.-J. Kim, A. Sarkar, Md. K. Nazeeruddin, M. Gratzel, and S. I. Seok, Nat. Photonics **7**(6), 486–491 (2013).
[7] S. D. Stranks, G. E. Eperon, G. Grancini, C. Menelaou, M. J. P. Alcocer, T. Leijtens, L. M. Herz, A. Petrozza, and H. J. Snaith, Science **342**(6156), 341–344 (2013).
[8] G. Xing, N. Mathews, S. Sun, S. S. Lim, Y. M. Lam, M. Grätzel, S. Mhaisalkar, and T. C. Sum, Science **342**(6156), 344–347 (2013).
[9] C. Wehrenfennig, G. E. Eperon, M. B. Johnston, H. J. Snaith, and L. M. Herz, Adv. Mater. **26**(10), 1584–1589 (2014).
[10] V. D'Innocenzo, G. Grancini, M. J. P. Alcocer, A. R. S. Kandada, S. D. Stranks, M. M. Lee, G. Lanzani, H. J. Snaith, and A. Petrozza, Nat. Commun. **5**, 3586 (2014).
[11] J. M. Ball, M. M. Lee, A. Hey, and H. J. Snaith, Energy Environ. Sci. **6**(6), 1739–1743 (2013).
[12] J. Burschka, N. Pellet, S.-J. Moon, R. Humphry-Baker, P. Gao, M. K. Nazeeruddin, and M. Gratzel, Nature (London) **499**(7458), 316–319 (2013).
[13] A. Abrusci, S. D. Stranks, P. Docampo, H.-L. Yip, A. K. Y. Jen, and H. J. Snaith, Nano Lett. **13**(7), 3124–3128 (2013).
[14] J. H. Noh, S. H. Im, J. H. Heo, T. N. Mandal, and S. I. Seok, Nano Lett. **13**(4), 1764–1769 (2013).
[15] N. J. Jeon, J. Lee, J. H. Noh, M. K. Nazeeruddin, M. Grätzel, and S. I. Seok, J. Am. Chem. Soc. **135**(51), 19087–19090 (2013).
[16] G. E. Eperon, V. M. Burlakov, P. Docampo, A. Goriely, and H. J. Snaith, Adv. Funct. Mater. **24**(1), 151–157 (2014).
[17] B. Conings, L. Baeten, C. De Dobbelaere, J. D'Haen, J. Manca, and H.-G. Boyen, Adv. Mater. **26**(13), 2041–2046 (2014).
[18] M. Liu, M. B. Johnston, and H. J. Snaith, Nature (London) **501**(7467), 395–398 (2013).
[19] P. Docampo, J. M. Ball, M. Darwich, G. E. Eperon, and H. J. Snaith, Nat. Commun. **4**, 2761 (2013).
[20] J. You, Z. Hong, Y. Yang, Q. Chen, M. Cai, T.-B. Song, C.-C. Chen, S. Lu, Y. Liu, H. Zhou, and Y. Yang, ACS Nano **8**(2), 1674–1680 (2014).
[21] K. Kawano, R. Pacios, D. Poplavskyy, J. Nelson, D. D. C. Bradley, and J. R. Durrant, Sol. Energy. Mater. Sol. Cells **90**(20), 3520–3530 (2006).
[22] K. Wojciechowski, M. Saliba, T. Leijtens, A. Abate, and H. J. Snaith, Energy Environ. Sci. **7**(3), 1142–1147 (2014).
[23] A. Yella, L.-P. Heiniger, P. Gao, M. K. Nazeeruddin, and M. Grätzel, Nano Lett. **14**(5), 2591–2596 (2014).
[24] J. T.-W. Wang, J. M. Ball, E. M. Barea, A. Abate, J. A. Alexander-Webber, J. Huang, M. Saliba, I. Mora-Sero, J. Bisquert, H. J. Snaith, and R. J. Nicholas, Nano Lett. **14**(2), 724–730 (2014).
[25] A. Katoch, H. Kim, T. Hwang, and S. Kim, J. Sol-Gel Sci. Technol. **61**(1), 77–82 (2012).
[26] M. Saliba, K. W. Tan, H. Sai, D. T. Moore, T. Scott, W. Zhang, L. A. Estroff, U. Wiesner, and H. J. Snaith, "Influence of Thermal Processing Protocol upon the Crystallization and Photovoltaic Performance of Organic-Inorganic Lead Trihalide Perovskites," J. Phys. Chem. C (published online).
[27] J. F. Moulder, W. F. Stickle, P. E. Sobol, and K. D. Bomben, *Handbook of X-ray Photoelectron Spectroscopy* (Physical Electronics, Inc., Minnesota, USA, 1995).
[28] F. Werfel and O. Brummer, Phys. Scr. **28**(1), 92–96 (1983).
[29] NIST X-ray Photoelectron Spectroscopy Database, Version 4.1, http://srdata.nist.gov/xps/
[30] G. K. Wertheim and S. B. Dicenzo, J. Electron Spectrosc. **37**(1), 57–67 (1985).
[31] C. De Dobbelaere, J. Mullens, A. Hardy, and M. K. Van Bael, Thermochim. Acta **520**(1–2), 121–133 (2011).
[32] D. Liu and T. L. Kelly, Nat. Photon. **8**(2), 133–138 (2014).

This article is copyrighted as indicated in the article. Reuse of AIP content is subject to the terms at: http://aplmaterials.aip.org/about/rights_and_permissions Downloaded to IP: 37.201.224.142 On: Thu, 17 Jul 2014 17:27:10